MAGNETIC RESONANCE IN CHEMISTRY
Magn. Reson. Chem. **36**, 892–900 (1998)

Fluorine-19 MAS and $^1H \rightarrow {}^{19}F$ CP/MAS NMR studies of Viton fluoropolymers

Gustavo A. Monti† and Robin K. Harris*

Department of Chemistry, University of Durham, South Road, Durham DH1 3LE, UK

Received 19 January 1998; revised 1 June 1998; accepted 16 June 1998

ABSTRACT: Fluorine-19{^{1}H} nuclear magnetic resonance (NMR) at 188.29 MHz, including $^1H \rightarrow {}^{19}F\{^1H\}$ cross-polarization (CP) with high-speed magic-angle spinning (MAS), was used to study some fluoropolymers of the Viton type. The systems examined were (a) copolymers of vinylidene fluoride and hexafluoropropene and (b) terpolymers of vinylidene fluoride, tetrafluoroethene and hexafluoropropene. Both commercial and specially prepared samples were used. Different $^1H \rightarrow {}^{19}F\{^1H\}$ CP/MAS experiments were applied to study the relaxation of the polymers. The results are discussed in terms of the CP dynamics, using parametrized equations. © 1998 John Wiley & Sons, Ltd.

KEYWORDS: NMR; ^{19}F NMR; solid; Viton; fluoropolymers; cross-polarization; magic-angle spinning

INTRODUCTION

The magic-angle spinning (MAS) technique has proved to be of immense value in the structural characterisation of solid polymers. Usually it has been applied to ^{13}C NMR, in conjunction with cross-polarization (CP) from protons and high-power decoupling of protons.

The existence of ^{19}F in fluoropolymers in principle opens up new possibilities for high-resolution NMR, but for solids surprisingly little work has been done until recently. This situation may be traced to the fact that, whenever the solid also contains hydrogen, high-power ^{1}H decoupling is usually expected to be required to eliminate the effects of (^{1}H,^{19}F) dipolar interactions from ^{19}F spectra. Moreover, it is desirable to use CP from ^{1}H to ^{19}F (and vice versa), allowing selective and discriminating experiments to be implemented. However, ^{1}H and ^{19}F frequencies differ by only *ca.* 6%, so very effective electronic filtering is required, and this has inhibited spectroscopists from attempting the experiments. Suitably robust probes are, fortunately, now available and we, with others, have been exploiting high-resolution ^{19}F solid-state NMR in studies of solid fluoropolymers[1–5] and other proton-containing fluorinated solids.[4,6,7]

Most commercial cured fluorocarbon elastomers are solvent resistant. Hence it is important to achieve ^{19}F high-resolution solid-state spectra of these polymers in order to understand their microstructure directly in the state in which they have practical applications.

Dec *et al.*[8] studied copolymers of vinylidene fluoride (VDF) and hexafluoropropene (HFP), copolymers of VDF and chlorotrifluoroethene (CTFE) and terpolymers of VDF, tetrafluoroethene (TFE) and HFP. They demonstrated the feasibility of obtaining ^{19}F high-resolution solid-state spectra, at room temperature, of these samples using direct polarization and MAS speeds of about 18 kHz, without the requirement of proton decoupling. This situation arises because of the high mobility at the molecular level in these systems, which is inherent in their elastomeric nature. Thus, Dec *et al.*[8] were able to make assignments of chemical shifts in terms of five-carbon sequences (pentads). Isbester *et al.*[9] combined very high-speed MAS with high temperature operation to improve resolution in ^{19}F solid-state NMR spectra of fluoropolymers.

As far as we know, apart from work in our laboratory,[1,3–5] no previous studies have been reported applying $^1H \rightarrow {}^{19}F\{^1H\}$ CP/MAS techniques in the study of fluorocarbon elastomers. In this work we applied direct polarization and cross-polarization techniques (especially measurements of relaxation times) in order to obtain additional information about chemical structure, molecular-level mobility and heterogeneity in fluoropolymers of the types VDF–HFP and VDF–HFP–TFE. These are frequently referred to as Viton. We have also directed our attention towards the measurement of spin relaxation properties for these systems.

EXPERIMENTAL

Samples

In this work we examined copolymers and terpolymers of the Viton type, both commercial in origin and specially prepared samples. Viton A is a random copolymer of CF_2CH_2 and CF_3CFCF_2, although with a

---

* *Correspondence to*: R. K. Harris, Department of Chemistry, University of Durham, South Road, Durham DH1 3LE, UK.
E-mail: r.k.harris@durham.ac.uk

† Permanent address: Facultad de Matemática, Astronomía y Física, Universidad Nacional de Córdoba, Ciudad Universitaria, 5000 Córdoba, Argentina.

Contract/grant sponsor: UK Engineering and Physical Sciences Research Council; *Contract/grant number*: GR/L02906.

CCC 0749-1581/98/120892–09 $17.50

restriction that adjacent CF_3CFCF_2 repeated units are not expected. Viton B is a terpolymer containing CF_2CF_2 units also. A commercial sample of Viton A (I) was purchased from Goodfellow (Cambridge, UK). This sample is a black sheet 2–3 mm thick, with density 2.0 g cm^{-3}, lower working temperature -10 to -50 °C and upper working temperature 220–300 °C. It is a cured polymer, containing a variety of additives, the precise composition being unknown to us. On the other hand, a sample of Viton A (II) and another of Viton B (III) were prepared at the University of Durham by members of the Interdisciplinary Research Centre in Polymer Science (IRC). The latter two samples do not contain any additives or a cure system (and so are soluble). The samples were ground into a powder under liquid nitrogen and dried under vacuum at 70 °C for 8 h prior to being packed in the rotor.

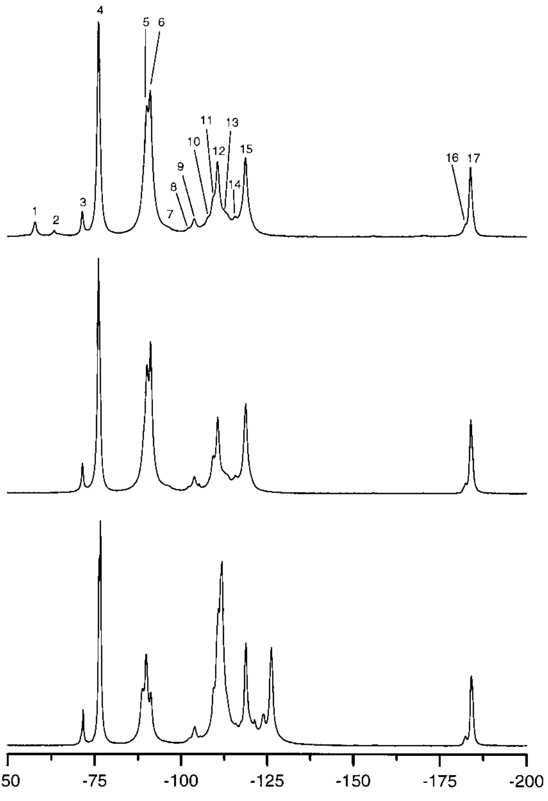

Figure 1. Fluorine high-resolution solid-state NMR spectra of Viton. Top, commercial sample of Viton A (I); middle, sample of Viton A (II); bottom, sample of Viton B (III). For detection the direct polarization technique without proton decoupling during acquisition was used. Spectrometer operating conditions: spin rate, 15 kHz; pulse duration, 3 μs for 90° pulse angle; recycle delay, 4 s; spectral width, 100 kHz.

Nuclear magnetic resonance

Solution-state NMR experiments were carried out on a Varian spectrometer operating at resonance frequencies of 399.96 and 376.29 MHz for protons and fluorine nuclei, respectively. Solution-state ^{19}F NMR spectra of samples II and III were recorded using direct polarization with proton decoupling. Deuterated acetone was used as solvent.

All solid-state NMR experiments were carried out on a Chemagnetics CMX 200 spectrometer operating at resonance frequencies of 200.13 and 188.29 MHz for protons and fluorine nuclei, respectively. We used a commercial (Chemagnetics) $^1H,^{19}F$ double-tuned APEX MAS probe capable of high-power (up to *ca.* 100 kHz) heteronuclear decoupling, with 4 mm o.d. zirconia Pencil rotors. Samples were restricted to the central 12 mm length of the rotors. Vespel drive tips, spacers and end caps were utilised to avoid any unwanted background signal on the fluorine channel. Samples were spun at the magic angle at rates between 10 and 15 kHz. Experiments were carried out at ambient probe temperature (*ca.* 297 K). Proton and fluorine field strengths were equivalent to 80 kHz for all experiments. Fluorine chemical shifts are quoted with respect to $CFCl_3$ and were measured via a sample of liquid C_6F_6 ($\delta_{C_6F_6} = -164.3$ ppm) without r.f. applied at the proton frequency.

The ^{19}F NMR spectra, with and without proton decoupling, were recorded using direct polarization with $\pi/2$ pulses of 3 μs duration. Relaxation delays of 4 s are sufficiently long to ensure quantitative peak intensities. In Fig. 1 ^{19}F NMR spectra obtained at a spinning speed of 15 kHz are shown.

Fluorine-19 spin–lattice relaxation times in the laboratory frame, T_1, and ^{19}F and ^1H spin–lattice relaxation times in the rotating frame, $T_{1\rho}$, were measured under high-resolution conditions (i.e. selectively). Relaxation times T_1 were obtained using the inversion–recovery technique (π–t–$\pi/2$–acq) and the ^{19}F $T_{1\rho}$ relaxation times were measured by means of the variable-time spin-lock technique. The ^1H $T_{1\rho}$ data were derived via ^{19}F resonance by a variable ^1H spin-lock followed by $^1H \rightarrow {}^{19}F$ cross-polarization. In some cases decoupling of the complementary nucleus was implemented during the variable time allowed for relaxation. The cross-polarization dynamics were studied using both the standard (variable contact time) CP sequence and a pulse sequence introduced by Tekely *et al.*[10] called TORQUE (TOneRhoQUEnching) (Fig. 2). In the standard analysis of a variable-contact CP experiment, two simultaneous processes, the build-up of spin magnetization for the observed nuclei (a local process but modified by proton spin diffusion) and the ^1H spin relaxation in the rotating frame, are taken into account. It is sometimes difficult to disentangle these two processes and to evaluate the cross-polarization rate alone. This problem may be circumvented by using the TORQUE pulse sequence. However, the situation is more complicated for $^1H \rightarrow {}^{19}F$ CP when fluorine spin–lattice relaxation in the rotating frame occurs at a significant rate. The WISE (two-dimensional) experiment[11,12] is also applicable to fluoropolymers containing protons. This yields data on proton bandshapes relevant to particular fluo-

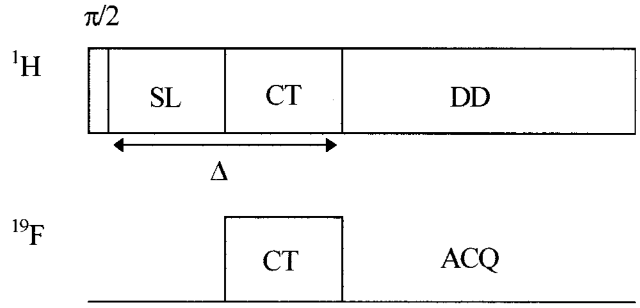

Figure 2. TORQUE pulse sequence for analysing CP data without the complications introduced by proton $T_{1\rho}$. The value of Δ is kept constant while the contact time is varied.

rine resonances (provided short contact times are used to minimize spin diffusion effects). If fluorine decoupling is employed during the evolution time, t_1, then the proton dimension yields (^{1}H,^{1}H) dipolar second moments, whereas without such decoupling the second moments contain both (^{1}H,^{19}F) and (^{1}H,^{1}H) contributions.[3,13]

RESULTS AND DISCUSSION

Following the work of Dec *et al.*[8] and solution-state NMR studies,[14,15] we have assigned chemical shifts to structural features. The results are given in Table 1. The peaks indicated with a question mark in Table 1 do not correspond to any known or possible pentads for this kind of copolymer. They may perhaps be attributed to resonances of unsaturated monomer units.[16] Our ^{19}F NMR solution-state spectra of samples II and III were used in the assignment of peaks for these polymers. For the commercial sample I an analysis of the relative ^{19}F signal intensities was made. Lorentzian lineshapes, in a computer deconvolution of the ^{19}F spectrum, were used to simulate the peaks. Relative integrated intensities for each peak of the sample are given in Table 1. The analysis of the intensities determines the composition as VDF:HFP = 78:22. Resolution in the ^{19}F spectra is not improved by application of r.f. proton decoupling at ambient temperature. In this kind of rubbery sample a spinning speed of about 10 kHz, combined with molecular-level motion of the polymer chains, is sufficient to average (^{1}H,^{19}F) dipolar interactions efficiently. However, the Bloch–Siegert effect[17] results in the chemical shifts for decoupled spectra appearing *ca.* 1.7 ppm to low frequency of the corresponding shifts in coupled spectra.

The relaxation behaviour for samples I, II and III can be described as follows. The ^{19}F relaxation times in the laboratory frame all show single-exponential decay of the magnetization as a function of the relaxation delay, with a value of 0.40 ± 0.01 s in all three samples and for all the resolved lines (whether they are associated with VDF, TFE or HFP units). We conclude that spin diffusion is effective enough to produce a single $T_1{}^{\mathrm{F}}$ value over the entire sample. Fluorine and proton relaxation times in the rotating frame are reported in Table 2. The results were unchanged when decoupling was applied to the complementary nucleus during detection. The relaxation times $T^{\mathrm{F}}_{1\rho}$ for the lines associated with CF/CF$_3$ of the HFP units (resonances at −71, −75 and −184 ppm) are slightly but significantly higher than for those associated with CF$_2$ fluorines, so that fluorine spin diffusion is not fully effective for spin–lattice relaxation in the rotating frame. This is presumably due, at least in part, to the resolution in the ^{19}F spectrum, which restricts spectral spin diffusion. However, in spite of this,

Table 1. Peak deconvolution and structural assignment of commercial sample I of Viton A

Peak No.[a]	Chemical shift,[b] δ_{F} (ppm)	Area (%)	Structural assignment[c]
1	−57.8	1.4	?
2	−63.3	0.5	?
3	−71.4	1.5	HTXTH (CF$_3$)
4	−76.1	20.4	TTXHT (CF$_3$)
5–6	−90.0, −91.2	32.9	THTHT
7	−96.2	1.8	HHTHT
8–9	−102.2, −103.8	2.2	THTXT
10–13	−107.9 to −112.7	18.5	THTTX XHTTX
14	−115.9	1.9	HTTHH
15	−118.8	11.5	HTTXH
16	−182.2	0.5	HTXTH (CF)
17	−184.0	6.9	TTXHT (CF)

[a] See Fig. 1.

[b] No proton decoupling was applied during acquisition of the spectra, so corrections for the Bloch–Siegert shift are not required.

[c] H = —CH$_2$—, T = —CF$_2$—, X = —CF(CF$_3$)—.

Table 2. Proton and fluorine spin–lattice relaxation times in the rotating frame for the three Viton samples, measured at a spin-lock field of 80 kHz

Sample	Peak position (ppm)	^{19}F $T_{1\rho}$ (ms) (±0.1 ms)	^{1}H $T_{1\rho}$ (ms) (±0.1 ms)
Viton A (I)	−71	1.4	–
	−75	1.6	1.1
	−90	1.0	1.2
	−110	0.9	1.2
	−118	0.8	0.9
	−184	1.6	1.3
Viton A (II)	−75	1.7	1.1
	−90	1.1	1.5
	−110	0.8	1.1
	−118	0.9	0.9
	−184	1.7	1.0
Viton B (III)	−76	1.9	1.1
	−90	1.1	1.4
	−112	1.0	1.2
	−120	1.1	1.1
	−126	1.4	1.2
	−185	2.0	1.0

the measured values of $T_{1\rho}^{F}$ are as short as those of $T_{1\rho}^{H}$. Some of the CF_2 signals have contributions from HFP units, which complicates the interpretation. The distinctive fluorine $T_{1\rho}$ relaxation of the CF_3 group may be attributed to the internal rotation of the group around the C—C axis. Suppose relaxation arises from F–F dipole–dipole interactions within the CF_3 group and that CF_3 internal rotation is rapid compared with backbone motion. Then the correlation time is reduced by a factor of $(3\cos^2\Delta - 1)^2/4$, where Δ is the angle between the rotation axis and the F–F vector. For the CF_3 group $\Delta = 90°$ and the reduction factor is 1/4. Additionally the number of geminal F–F interactions for CF_3 groups is 2 and for CF_2 groups it is 1. Hence we expect a ratio $T_{1\rho}(CF_3)/T_{1\rho}(CF_2) \approx 2$, as observed. The longer $T_{1\rho}$ value for the CF peak is presumably due to longer F–F distances. However, there is a complication in this interpretation because preliminary 2D ^{19}F–^{19}F exchange experiments show a noticeable correlation between the CF and CF_3 resonances even for short mixing times (*ca.* 0.8 ms). Proton $T_{1\rho}$ relaxation times associated with all the ^{19}F peaks show similar values (probably equal within experimental error), as expected because there is only a narrow range of chemical sites for protons (only CH_2 groups, all adjacent to at least one CF_2 group) and the sample is morphologically homogeneous.

All CP experiments carried out in this work were performed at a high MAS speed, $\omega_r/2\pi = 10$ kHz. When ω_r exceeds the dipolar coupling frequencies, the Hartmann–Hahn match, $\omega_{1H} = \omega_{1F}$, is converted to a series of sidebands at $\omega_{1F} = \omega_{1H} \pm n\omega_r$, where ω_{1H} and ω_{1F} are measures of the radiofrequency field strengths of proton and fluorine nuclei ($\gamma_H B_{1H}$ and $\gamma_F B_{1F}$), respectively. The Hartmann–Hahn matching[18] profile was examined at proton r.f. amplitudes of 50 and 60 kHz while the fluorine r.f. amplitude varied from 40 to 80 kHz. The spinning speed was 10 kHz. The conventional CP sequence was used with a contact time of 1 ms. We observed the expected split of the apparent matching condition, as is the case when the spinning speed is comparable to, or greater than, the linewidth of the 'abundant' nuclei. Figure 3 shows the matching profiles for the different fluorine resonances. It is observed that CP, under the conditions used, is more efficient at the exact Hartmann–Hahn matching condition than at the sideband matching, which is contrary to the usual case in ^{1}H → ^{13}C CP/MAS experiments. Also, we observed that some sideband matching conditions, e.g. at the −1 and +2 sidebands, give very low or null intensity, producing a noticeably asymmetric profile. In Fig. 4 we compare the matching profile obtained using a standard CP sequence with that from a ramped-amplitude[19] CP sequence (size of the ramp 40 kHz in steps of 0.6 kHz).

The evolution of the ^{19}F magnetization obtained from the standard CP experiment (at exact Hartmann–Hahn match) is shown in Fig. 5 as a function of the contact time, t_{CT}. The maximum intensity of the magnetization is reached around 900 μs. This relatively short value occurs in spite of the high mobility of the polymer and even when the ^{19}F–^{1}H dipolar coupling is additionally averaged by MAS. This is presumably because we are dealing with two abundant nuclei and with similar and strong dipolar couplings, resulting in an effective magnetization transfer process.

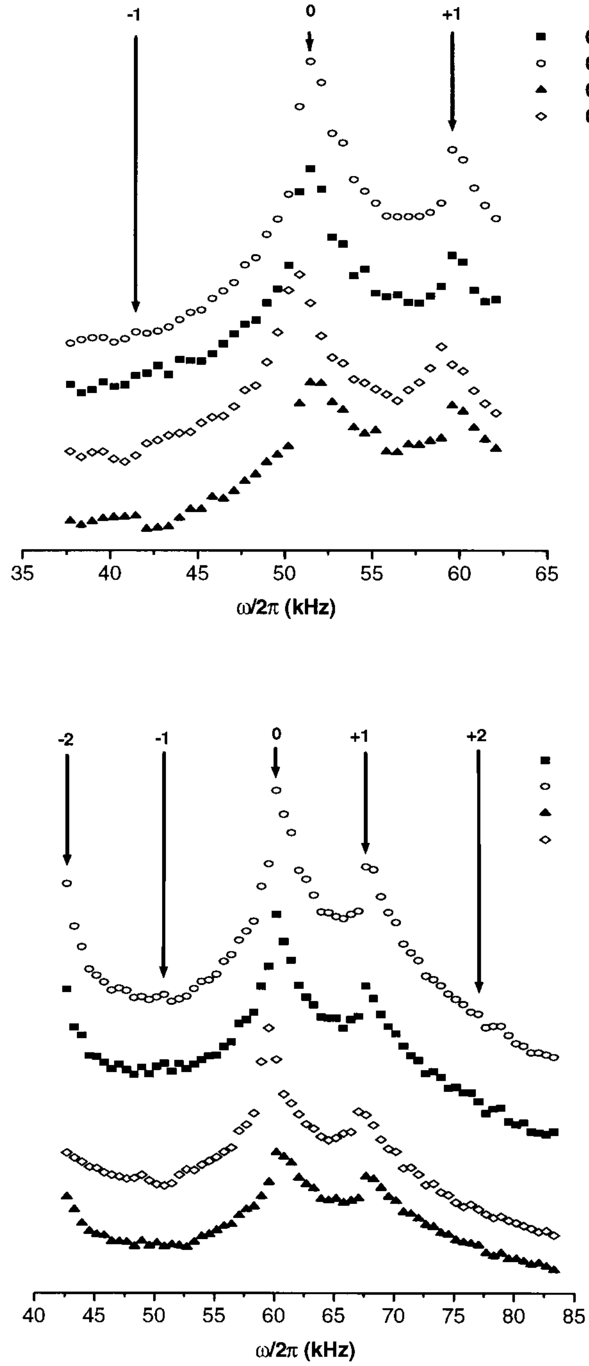

Figure 3. Cross-polarized intensity *vs.* ^{19}F field strength (expressed as ω_{1F}) for a sample of Viton A (II) obtained using the standard CP sequence. Spectrometer operating conditions: $\omega_{1H}/2\pi$ = (top) 50 and (bottom) 60 kHz; contact time, 1 ms; spin rate, 10 kHz.

To our knowledge, there has been little or no discussion of ^{1}H → ^{19}F CP dynamics in the literature, largely because of the complications inherent in treating two abundant spin baths. Usually, in considering the

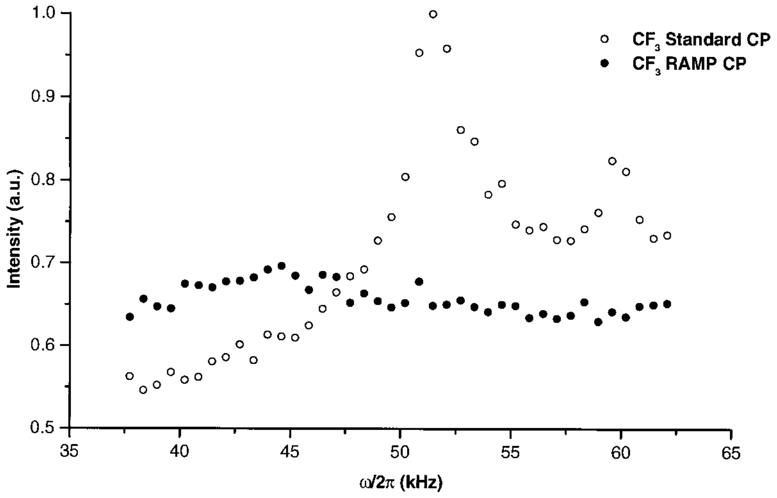

Figure 4. Cross-polarized intensity *vs.* ^{19}F field strength (expressed as $\omega_{1\mathrm{F}}$) for a sample of Viton A (II) obtained using (○) the standard CP sequence and (●) ramped-CP sequence. Only results for the -75 ppm fluorine resonance are shown. Spectrometer operating conditions: $\omega_{1\mathrm{H}}/2\pi = 50$ kHz; size of the ramp, 40 kHz; step size, 0.6 kHz; contact time, 1 ms; spin rate, 10 kHz.

description of CP processes between two nuclear spin species, I and S, the I spins are assumed to be abundant and the S spins rare, so that S–S interactions may be ignored, and it is valid to treat the system as an ensemble of subsystems, each consisting of a single S spin and a large number of I spins. Clearly this is not the case when I and S are protons and fluorines, respectively, and especially if they are present in comparable amounts as in some fluoroelastomers. In spite of this limitation, the evolution of the ^{19}F magnetization as a function of the contact time may be represented by the expression

$$M(t) \propto \exp\left(-\frac{t}{x}\right) - \exp\left[-\left(\frac{1}{y} + \frac{1}{T_{1\rho}^{\mathrm{F}}}\right)t\right] \qquad (1)$$

which is similar to that normally used[20] for cross-polarization to a dilute spin but with the addition of the term in $T_{1\rho}^{\mathrm{F}}$. Since this equation ignores the influence of the atomic ratio $N_{\mathrm{F}}/N_{\mathrm{H}}$, it may be regarded simply as a way of parametrising the CP dynamics, though in an ideal case x would be equated to $T_{1\rho}^{\mathrm{H}}$ and y to T_{HF}. It should also be noted that the differing values of $T_{1\rho}^{\mathrm{F}}$ for different groups implies there are several fluorine spin baths, which we have assumed to be independent—a condition that is unlikely to be fulfilled. To fit the experimental data to Eqn (1) the values for the parameter $T_{1\rho}^{\mathrm{F}}$ were taken from Table 2. Therefore, only two parameters (apart from a scaling factor), namely x and y, were varied in the fitting procedure. The values obtained are given in Table 3. It may be noted that $T_{1\rho}^{\mathrm{F}}$ is not much greater than y (cf. T_{HF}), so that fixing the former by a separate experiment when using Eqn (1) is essential.[21] The description of the data by Eqn (1) is acceptable, as can be seen from Fig. 5. However, since the parameters x and y given in Table 3 should not be regarded as the correct values of these $T_{1\rho}^{\mathrm{H}}$ and T_{HF}, respectively, it is not surprising that there is some discrepancy between $T_{1\rho}^{\mathrm{H}}$ data obtained by the variable spin-lock technique and the values of x given by variable contact-time CP experiments. Moreover, it may be noted that all the ^{19}F resonances show similar (although not identical) apparent cross-polarization rates (characteristic times y between 0.5 and 0.9 ms), even though the peaks at -75 and -184 ppm correspond to fluorine nuclei in HFP units (which have no protons).

Table 3. Parameters obtained from CP/MAS variable contact time experiments by fitting the data to Eqn (1) (using the fluorine $T_{1\rho}$ data determined by direct measurement)

Sample	Peak position (ppm)	x (ms)[a] ($\pm$0.1 ms)	y (ms)[b] ($\pm$0.2 ms)
Viton A (I)	-75	2.2	0.9
	-90	1.6	0.8
	-110	1.2	0.6
	-118	1.3	0.6
	-184	2.4	0.6
Viton A (II)	-76	3.1	0.7
	-91	2.2	0.6
	-111	1.5	0.5
	-119	1.4	0.5
	-185	2.8	0.7
Viton B (III)	-77	3.3	0.8
	-90	2.2	0.9
	-112	2.0	0.6
	-119	1.7	0.4
	-126	2.0	0.5
	-185	3.2	0.7

[a] A parameter reflecting $T_{1\rho}^{\mathrm{H}}$ (see text).
[b] A parameter reflecting T_{HF} (see text).

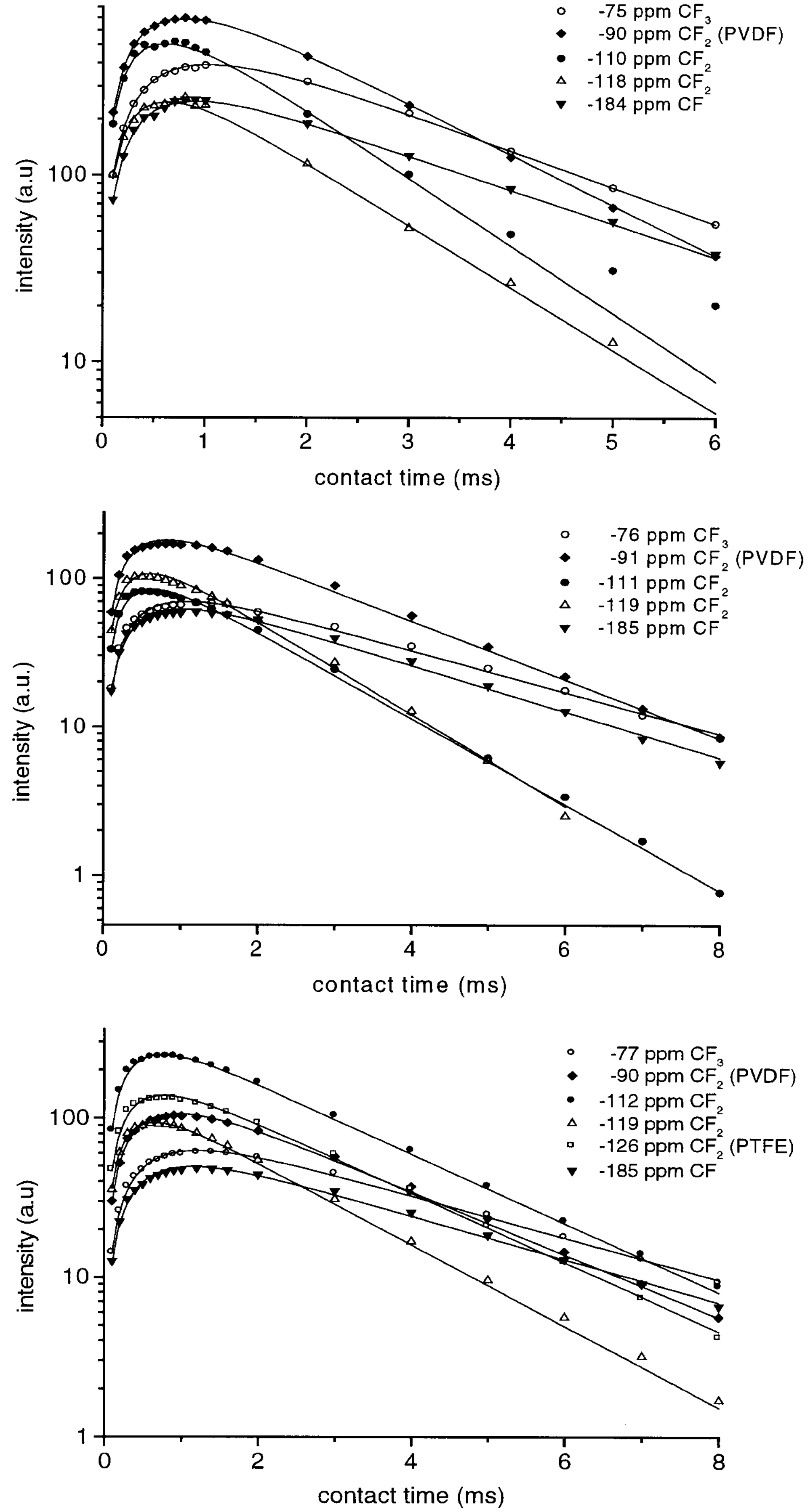

Figure 5. Evolution of the ^{19}F magnetization as a function of the contact time in a standard cross-polarization experiment. Top, commercial sample of Viton A (I); middle, sample of Viton A (II); bottom, sample of Viton B (III). The solid lines were obtained by fitting the experimental data to Eqn (1).

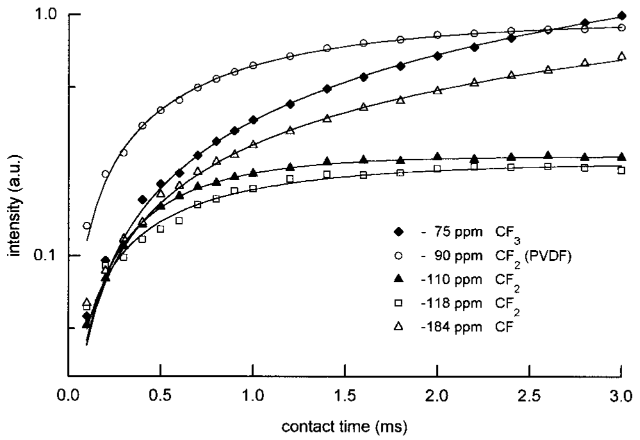

Figure 6. Contact-time dependence of the ^{19}F signal intensity for a TORQUE experiment on the commercial sample of Viton (I). The constant time $t_{SL} + t_{CT} = 3$ ms was used throughout. The solid lines were obtained by fitting the experimental data to Eqn (2).

Table 4. Parameters for Viton A (I) obtained from TORQUE experiment by fitting the data to Eqn (2) (using the directly measured values for proton and fluorine $T_{1\rho}$).

Peak position (ppm)	z (ms)[a]
-75	3.2 ± 0.1
-90	1.0 ± 0.1
-110	0.6 ± 0.1
-118	0.6 ± 0.1
-184	5 ± 1

[a] A parameter reflecting T_{HF}.

The experimental data obtained using the TORQUE sequence[10] reveal with more detail the evolution of the ^{19}F magnetisation (Fig. 6). They clearly show that the peaks associated with CF and CF$_3$ fluorines gain magnetization more slowly than the peaks associated with CF$_2$ groups. The TORQUE experimental data for the commercial sample I were fitted using the following expression:[10]

$$M(t_{SL}, t_{CP}) \propto \exp\left(-\frac{3.0}{T_{1\rho}^{H}}\right) - \exp\left[-\left(\frac{1}{z} + \frac{1}{T_{1\rho}^{F}}\right)t_{CP} - \frac{3.0 - t_{CP}}{T_{1\rho}^{H}}\right] \quad (2)$$

where $t_{CP} + t_{SL} = 3.0$ ms. As for Eqn (1), the time constant z merely represents a way of parametrizing the

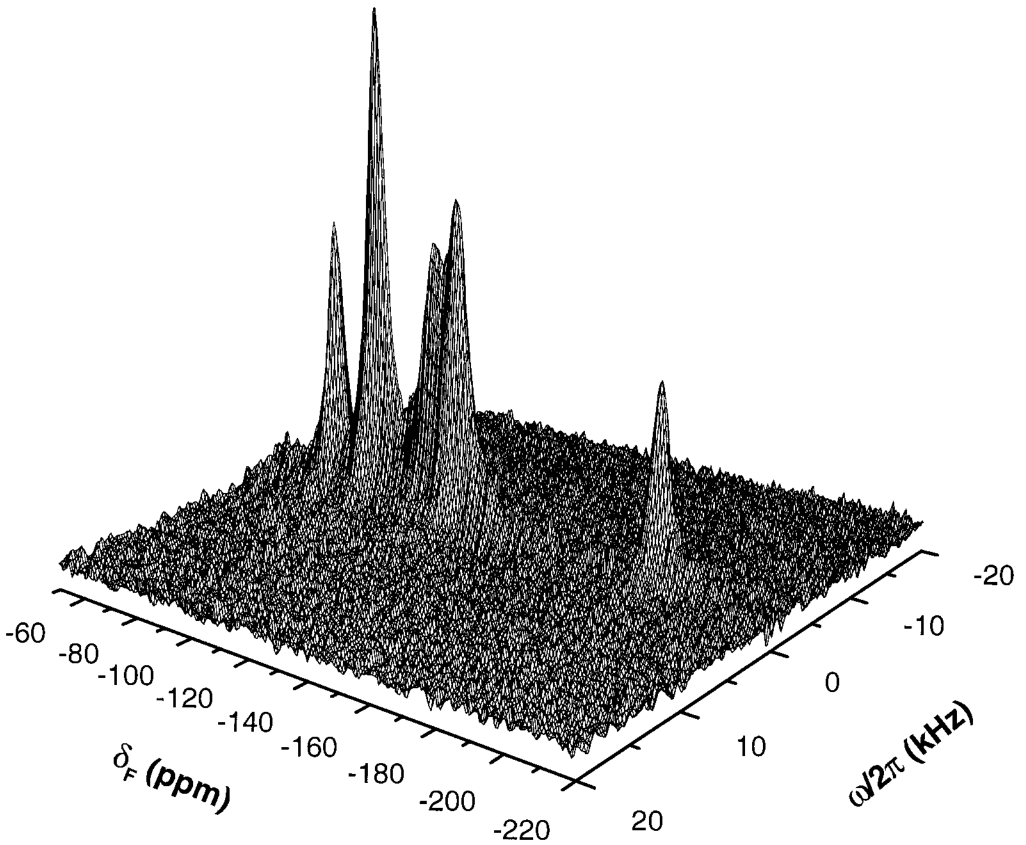

Figure 7. Stacked plot for a proton–fluorine WISE experiment for the commercial Viton sample I, with ^{19}F decoupling during the evolution time t_1. Spectrometer operating conditions: contact time, 50 μs; spin rate, 10 kHz; 128 points in t_1 with 10 μs increments; pulse power in both channels, equivalent to 3 μs for 90° pulse angles; recycle delay, 3 s.

process and should not be taken to represent accurately the true variable T_{HF}.

The two variable parameters of this equation are a scaling factor and z (when the values for proton and fluorine rotating-frame relaxation times are taken to be those obtained by variable spin-lock techniques from independent experiments). The values of z obtained by fitting the experimental TORQUE data to Eqn (2) are given in Table 4. In fact, Eqn (2) provides a very good description of the evolution of fluorine magnetization (Fig. 6). From Table 4 we can see that effective T_{HF} values (z) for the peaks at -90, -110 and -118 ppm are very close to those obtained from the standard CP/MAS experiment, but for the peaks at -75 and -184 ppm (CF_3 and CF groups) the CP rates derived from the TORQUE data are much slower. The discrepancy between the $T_{1\rho}^{H}$ values obtained by the variable spin-lock technique and the apparent values x from variable contact-time CP are also more noticeable for the resonances at -75 and -184 ppm. As implied by Tekely *et al.*,[10] the increase in fluorine magnetization for long contact times, in the standard CP experiment, is responsible for this discrepancy. Owing to the slow CP build-up of fluorine magnetization, apparently slower $T_{1\rho}^{H}$ decays are observed in the standard CP experiments. Use of the TORQUE experiment makes the discrepancy more understandable and shows clearly that the CP process is less efficient for the signals at -75 and -184 ppm than for those of the CF_2 groups, perhaps again because of motional effects.

We are currently pursing further experimental and theoretical approaches in an attempt to understand the ^{1}H → ^{19}F CP dynamics in systems where both protons and fluorine nuclei are abundant.

It is known that copolymers of VDF and HFP can show some degree of crystallinity. The crystallinity is decreased as the amount of HFP in the copolymer is increased.[22–25] However, our $T_{1\rho}$ and WISE results do not discriminate between amorphous and crystalline phases of the copolymer studied. Figure 7 shows a WISE stacked plot, obtained with ^{19}F decoupling during t_1, for the commercial sample of Viton. There is no significant difference in this case in the proton linewidth associated with different ^{19}F chemical shifts, as expected with a single type of chemical site for protons and efficient proton spin diffusion. The proton second moments (including heteronuclear dipolar coupling) as obtained from the WISE experiment are about 70 (kHz)^2 for sample I but only 40 (kHz)^2 for samples II and III, in agreement with the influence of curing, which imparts some rigidity to the polymer. Applying ^{19}F decoupling during the evolution time caused no changes for samples II and III, but for sample I the second moment is reduced to *ca.* 40 (kHz)^2.

CONCLUSIONS

A series of Viton type fluoropolymers were studied using solid-state NMR, with ^{19}F direct-polarization MAS and ^{1}H → ^{19}F CP/MAS high-speed techniques. Resolution in the ^{19}F spectra is not improved by application of r.f. proton decoupling at ambient temperature. In this kind of rubbery sample, a spinning speed of about 10 kHz, combined with molecular-level motion of the polymer chains is sufficient to average (^{1}H,^{19}F) dipolar interactions efficiently. WISE experiments carried out with and without ^{19}F decoupling during the evolution time also indicate a weak effect of the (^{1}H, ^{19}F) dipolar interaction on the proton linewidth.

Similar ^{19}F T_1 values were obtained for all the resolved lines, whether they are associated with VDF, TFE or HFP units. We conclude that spin diffusion is effective enough to produce a single T_1 value over the entire sample. The relaxation times $T_{1\rho}$ (^{19}F) for the lines associated with CF/CF_3 of the HFP units (resonances at -71, -75 and -184 ppm) are slightly higher than for those associated with CF_2 fluorines. Proton $T_{1\rho}$ relaxation times associated with all the ^{19}F peaks show similar values, as expected because of the chemical nature of the sample.

The evolution of the ^{19}F magnetization, as a function of the contact time, in the ^{1}H → ^{19}F CP/MAS experiments is well described by the usual expression (1) in spite of the physical restrictions imposed by the system itself. Analysis of the TORQUE experimental data using Eqn (2) gives additional insights. As was mentioned by Tekely *et al.*,[10] use of the TORQUE technique helps to evaluate and understand CP rates.

The different experiments carried out do not detect any heterogeneity (i.e. no different, mobile and rigid, phases) for the three different Viton-type polymers studied.

Acknowledgements

G.A.M. is grateful to the Consejo Nacional de Investigaciones Científicas y Técnicas of Argentina (CONICET) for a postdoctoral research fellowship. We thank Professor W. J. Feast for the samples of pure Viton A and Viton B. Financial support from the UK Engineering and Physical Sciences Research Council under grant GR/L0290b is gratefully acknowledged. We thank P. Holstein, S. Ando and the referees for helpful comments, which have resulted in an improved discussion of the experimental results.

REFERENCES

1. R. K. Harris, G. A. Monti and P. Holstein, in *NMR of Solid Polymers*, edited by I. Ando and T. Asakura, Section 6.6 and Chapter 18. Elsevier, Amsterdam, (1998).
2. R. K. Harris, S. A. Carrs, R. D. Chambers, P. Holstein, A. P. Minoja and U. Scheler, *Bull. Magn. Reson.* **17**, 37 (1995).
3. U. Scheler and R. K. Harris, *Solid State NMR* **7**, 11 (1996).
4. P. Holstein, R. K. Harris and B. J. Say, *Solid State NMR* **8**, 201 (1997).
5. P. Holstein, U. Scheler and R. K. Harris, *Polymer* **39**, 4937 (1998).
6. S. A. Carss, U. Scheler, R. K. Harris, P. Holstein and R. A. Fletton, *Magn. Reson. Chem.* **34**, 63 (1996).
7. S. A. Vierkötter, *J. Magn. Reson. A* **118**, 84 (1996).
8. S. F. Dec, R. A. Wind and G. E. Maciel, *Macromolecules* **20**, 2754 (1987).
9. P. K. Isbester, T. A. Kestner and E. J. Munson, *Macromolecules* **30**, 2800 (1997).
10. P. Tekely, V. Gérardy, P. Palmas, D. Canet and A. Retournard, *Solid State NMR* **4**, 361 (1995).

11. N. Zumbulyadis, *Phys. Rev. B* **33**, 6495 (1986).
12. K. Schmidt-Rohr, J. Claus and H. W. Spiess, *Macromolecules* **25**, 3273 (1992).
13. P. Tekely, P. Palmas and P. Mutzenhardt, *Macromolecules* **26**, 7363 (1993).
14. R. C. Ferguson, *Kautsch. Gummi Kunstst.* **18**, 723 (1965).
15. Y. M. Murasheva, A. S. Shashkov and A. A. Donstov, *Polym. Sci. USSR* (*Engl. Transl.*) **23**, 711 (1981).
16. R. K. Harris and P. Jackson, *Chem. Rev.* **91**, 1427 (1991).
17. F. Bloch and A. Siegert, *Phys. Rev.* **57**, 552 (1940).
18. S. R. Hartmann and L. E. Hahn, *Phys. Rev.* **128**, 2042 (1962).
19. G. Metz, X. Wu and S. O. Smith, *J. Magn. Reson. A* **110**, 219 (1994).
20. M. Mehring, *Principles of High Resolution NMR in Solids*, 2nd ed. of *NMR—Basic Principles and Progress*, Vol. 11. Springer, Berlin (1983).
21. W. E. J. R. Maas, *Doctoral Thesis*, Catholic University of Nijmegen (1992).
22. M. Latour and R. L. Moreira, *J. Polym. Sci., Part B: Polym. Phys.* **25**, 1717 (1987).
23. M. Latour and R. L. Moreira, *J. Polym. Sci., Part B: Polym. Phys.* **25**, 1913 (1987).
24. G. Moggi, P. Bonardelli and J. C. J. Bart, *Polym. Bull* **7**, 115 (1982).
25. M. Latour, K. Anis and R. M. Farias, *J. Phys. D: Appl. Phys.* **22**, 806 (1989).